Supporting Information

A Two-stage Energy Mediation via Salt and Glycine Programmed DNA-Engineered Crystals

Yanqiu Du[a,b], Xiang Zhou[c], Jing Jin*[a], Haojun Liang[c], Yongfeng Men[a], Wei Jiang*[a]

[a] *State Key Laboratory of Polymer Physics and Chemistry, Changchun Institute of Applied Chemistry, Chinese Academy of Sciences, Changchun, 130022, P.R. China*

[b] *College of Materials and Textile Engineering, Jiaxing University, Jiaxing, 314001, P.R. China*

[c] *Department of Polymer Science and Engineering, University of Science and Technology of China, Hefei, Anhui, 230026, P. R. China*

** Corresponding author: Fax: +86-431-85262126; Tel: +86-431-85262151;*

E-mail: wjiang@ciac.ac.cn; jjin@ciac.ac.cn;

1. Experimental section

Materials. All DNA oligonucleotides used were purchased from Sangon Biotechnology Co., Ltd (Shanghai, China). Thiolated oligonucleotides were purified using high-performance liquid chromatography (HPLC), while ULTRAPAGE for non-modified oligonucleotides Specific sequences used are listed in Table S1. All citrate-stabilized gold nanoparticles (~10 nm) were obtained from nanoComposix. Other chemicals were purchased from Aladdin Ltd. All of the materials were used directly without further purification.

Nanoparticle functionalization with DNA. Gold nanoparticle functionalization with DNA was conducted as previous literature procedures.[1] Briefly, thiolated oligonucleotides were reduced with 100 mM tris(2-carboxyethyl) phosphine hydrochloride (TCEP) (Sigma-Aldrich) for 1 h. Subsequently, excess TCEP was removed *via* a Sephadex G-25 column (GE Healthcare). Then oligonucleotides were directly added to nanoparticle solution and incubated overnight. After 16 h, the mixture was brought to 10 mM sodium phosphate buffer (pH 7.4) and 0.01 wt% SDS. In salt aging stepwise, the solution was brought to final concentration of 0.5 M NaCl by drop-wise adding 4.0 M NaCl in six times at least 8 h intervals and allowed to hold for 16 h to maximize DNA loading. After three centrifugations to remove unbound DNA chains, nanoparticles were redispersed in 0.5 M NaCl buffer and stored at 4°C.

The Preparation of DNA-engineered Crystals by directly changing the salt concentration in solution. In the binary-component system, Linker-X and Linker-Y strands were separately added to DNA-functionalized nanoparticles (typically at molar ratio of 300:1), and slowly cooled from 45°C to 25°C. After the treatment, all the experiments were kept at 25°C. Then two types of nanoparticle solutions were mixed at molar ratios of 1:1, and final nanoparticle concentration was 50 nM by adding 0.5 M

NaCl, 10 mM sodium phosphate buffer (pH 7.4) and SDS solution. The stock solution was incubated for 30 min. In the single-component system, Linker-A strands were directly added to DNA-functionalized nanoparticles at 25°C for 30 min. The black aggregates formed in both systems were washed repeatedly with various salt concentration solutions to remove excess buffer and SDS, and were redispersed in a stock solution of 0, 100, 125, 150, 175, 200, 300, 400, and 500 mM NaCl in H_2O for 24 h. Finally, these samples were transferred to 1.0 mm glass capillary tubes for SAXS measurements.

The Preparation of DNA-engineered Crystals by the two-stage energy. First, a series of 0, 0.1, 0.5, 1.0, 2.0, 3.0 M, and saturated Gly at various salt concentration solutions were prepared. After DNA linkers added to DNA-functionalized nanoparticles in 500 mM NaCl solution, black aggregates were formed within 30 min in both systems. These aggregates were washed repeatedly with a constant concentration of Gly in salt solution and were redispersed in these stock solutions for 24 h and characterized with SAXS measurements.

The kinetics experiment by the two-stage energy. In a kinetics experiment, to prevent samples from damaging by multiple exposures, several samples were prepared at the same experimental condition. In the binary-component system, after a saturated Gly solution of 300 mM NaCl added to these aggregates, parallel samples at different reaction times (5, 30, 120, 180, 300 and 480 s) were characterized with SAXS measurements. In single-component system, after a saturated Gly solution of 200 mM NaCl added to these aggregates, parallel samples at different reaction times (0, 3, 5, 8, 60 and 120 min) were characterized with SAXS measurements.

Small-angle X-ray scattering (SAXS) characterization. Small-angle X-ray scattering experiments were performed at beamline BL16B1 at SSRF, Shanghai, China. X-rays of wavelength 1.24 Å (10 keV) were used and the bull collagen fiber as a

standard was used to calibrate in this system. Each SAXS pattern obtained in the center of the sample was collected within 5 s. A CCD area detector was used to detect the scattered radiation and 1-dimensional SAXS data were obtained by radial averaging of the 2-dimensional scattering patterns. Then these data were transformed into profiles of scattering intensity as a function of scattering vector q, $q=4\pi\sin\theta/\lambda$, where θ is half of the scattering angle 2θ and λ is the wavelength of X-ray radiation. Dark current frames were subtracted from all data; scattering of buffer and DNA was negligible in this work.

Average crystalline domain sizes were calculated using the Scherrer formula:

$$t = \frac{0.9\lambda}{B\cos\theta}$$

where t is the diameter of the crystalline domain in angstroms (assuming a pseudo-spherical crystal domain shape), λ is the wavelength of X-ray radiation, θ is the diffraction angle associated with the q_0 peak, and B is the full angular width at half maximum of the q_0 peak.

Scanning electron microscopy (SEM) characterization. The assembled colloidal crystals were stabilized based on covalent DNA cross-linking according to literature methods[2]**.** Briefly, 10 mg 8-methoxypsoralen (8-MOP) was dissolved in 1mL of a mixture of ethanol and salt solution (v/v, 3:1), and the stock solution was sonicated for 5 min. Before 8-MOP addition, crystals were washed repeatedly with the original salt with the addition of Gly to remove unreacted DNA-functionalized nanoparticles, DNA, and the supernatant. Then 50 μL of the 8-MOP solution was added to the crystals, and the mixture was left on a shaker for 6 h, finally irradiated with UV light at 365 nm for 6 h to covalently cross-link DNA strands. After removing the supernatant, the crystals were washed with a mixture of ethanol and deionized water (v/v, 1:1) to remove excess 8-MOP and salt from the solution. Scanning electron microscopy was performed with

a Merlin (ZEISS). 10 μL of the sample was drop-cast on a clean Si wafer and dried in air. Images were taken with an electron beam energy of 1 kV and an emission current of 300 μA.

Other measurement methods. Transmission electron microscopy (TEM) measurement was performed on JEOL JEM-1400 at an accelerated voltage of 120 kV. 2 μL of the sample was deposited onto a copper grid covered by carbon film and dried under air. UV-visible spectroscopy was measured using a PerkinElmer Lambda 35 UV-vis spectrophotometer. Dynamic light scattering (DLS) experiments were performed using a ZetaSizer Nano ZS (Malvern Instruments). All the samples were equilibrated for 2 min at 25 °C to ensure that the changes belong to the Brownian motion and not to any thermal conversion. Circular dichroic (CD) spectroscopy was obtained at 25°C using a MOS-500 circular dichroism spectropolarimeter (Biologic, France). Energy-dispersive X-ray spectra (EDX) were recorded by XL 30 E-SEM, FEG, Micron FEI PHILIPS.

2. Supplementary Figures and Table

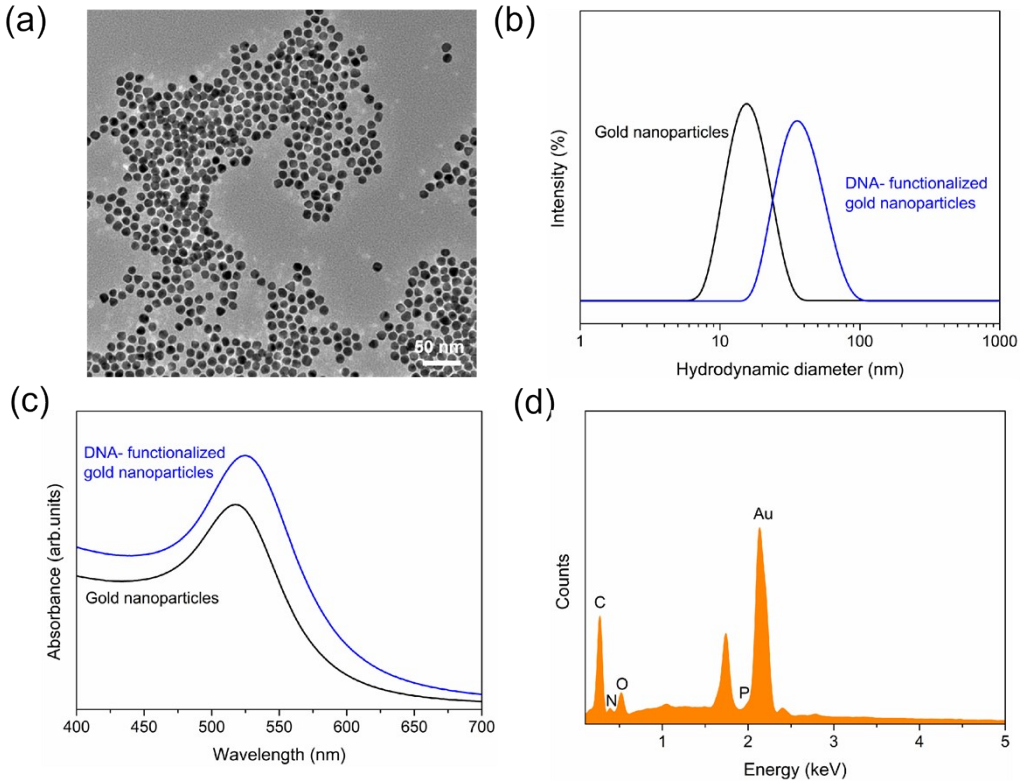

Fig. S1 (a) TEM images of DNA-functionalized gold nanoparticles; (b) Hydrodynamic diameters of bare gold nanoparticles and DNA-functionalized gold nanoparticles; (c) UV-Vis spectroscopy of bare gold nanoparticles and DNA-functionalized gold nanoparticles; (d) EDX spectroscopy of DNA-functionalized gold nanoparticles.

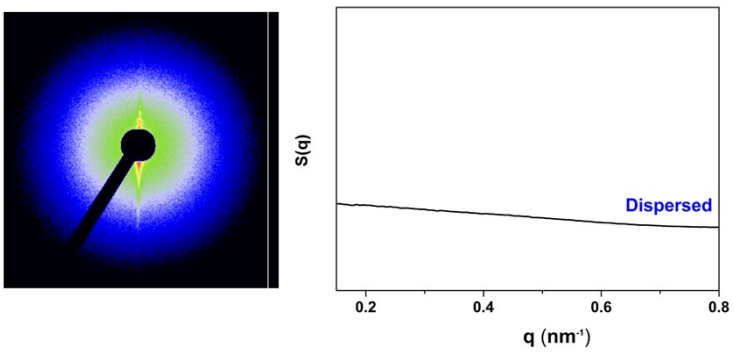

Fig. S2 SAXS patterns of dispersed nanoparticles without the addition of NaCl.

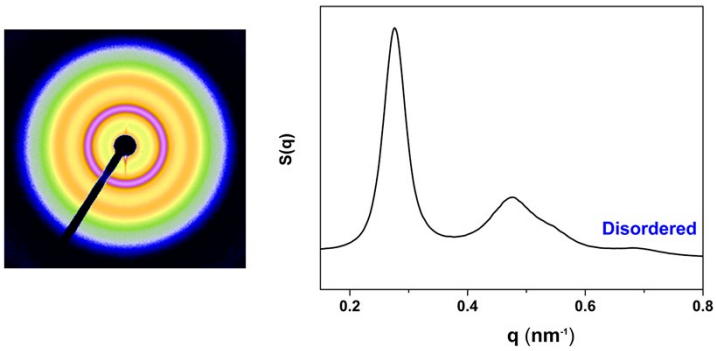

Fig. S3 SAXS patterns of disordered aggregates with the addition of 500 mM NaCl.

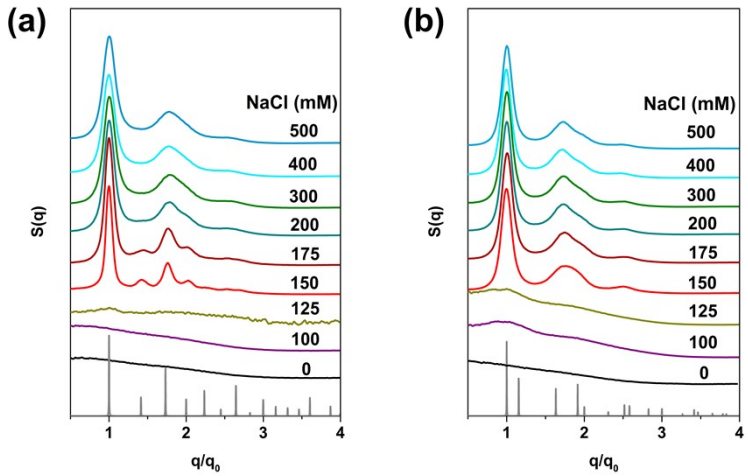

Fig. S4 SAXS profiles of the binary-component system (a) and the single-component system (b) in various concentrations of NaCl aqueous solutions from 500 to 0 mM. The gray lines at the bottom of (a) and (b) represent theoretical SAXS patterns for perfect BCC and FCC lattices.

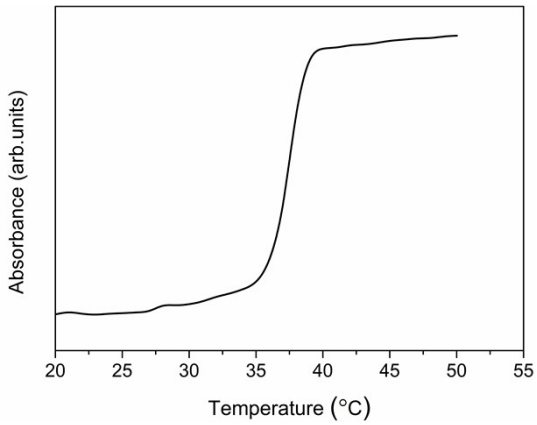

Fig. S5 Melting profile of binary-component aggregate determined by monitoring the absorbance change at 520 nm.

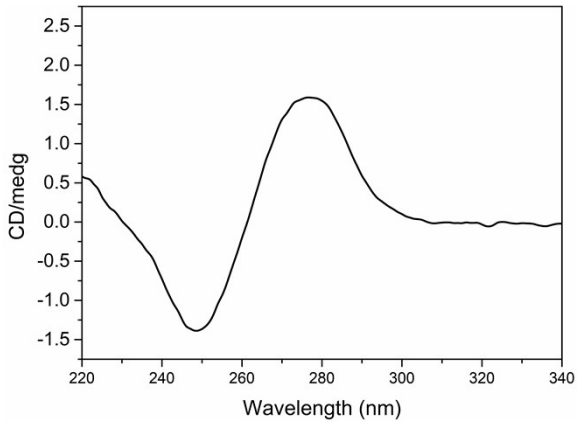

Fig. S6 Circular dichroism spectrum of dsDNA in a binary-component system.

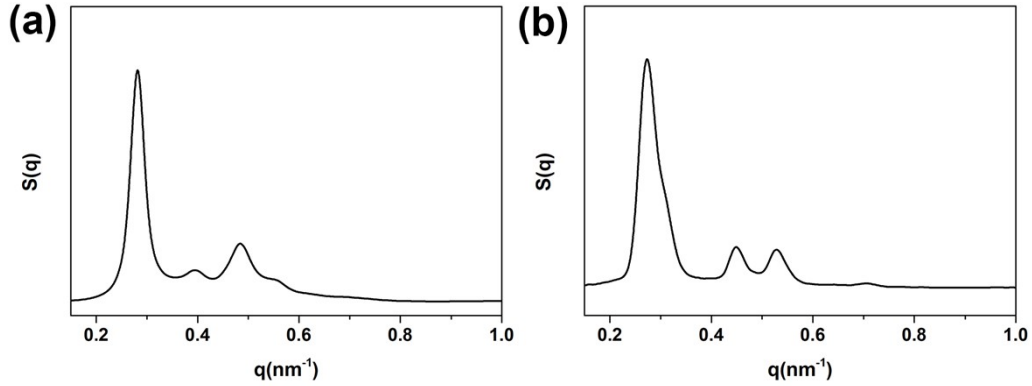

Fig. S7 Preparation of the crystals by the thermal annealing. SAXS pattern of annealing products in binary-component (a) and single-component systems (b). In the binary-component system, the disordered aggregates are cooled from 37°C to 25°C at a rate of 0.1°C/min. In the single-component system, the disordered aggregates are cooled from 45°C to 25°C at a rate of 0.1°C/min.

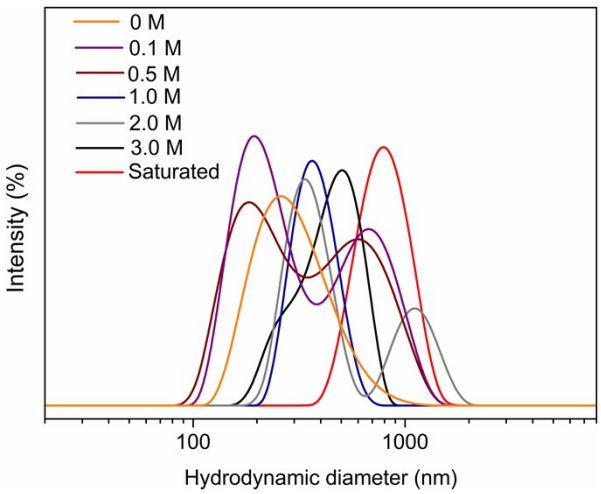

Fig. S8 Hydrodynamic diameters of aggregates with increasing Gly amount into 300 mM NaCl solution in the binary-component system by DLS measurements.

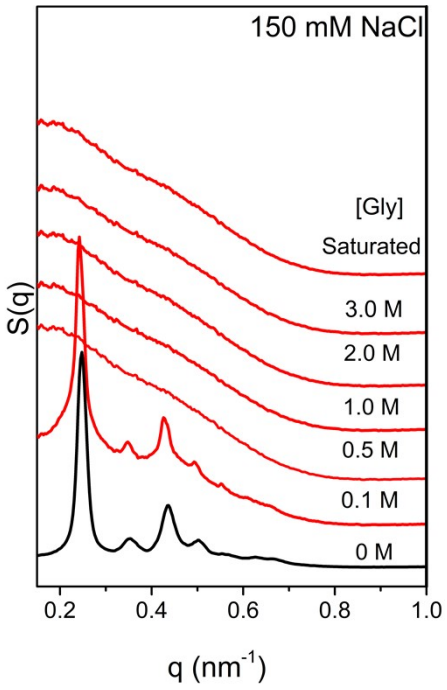

Fig. S9 SAXS data for aggregates with increasing Gly amount into 150 mM NaCl solution in the binary-component system.

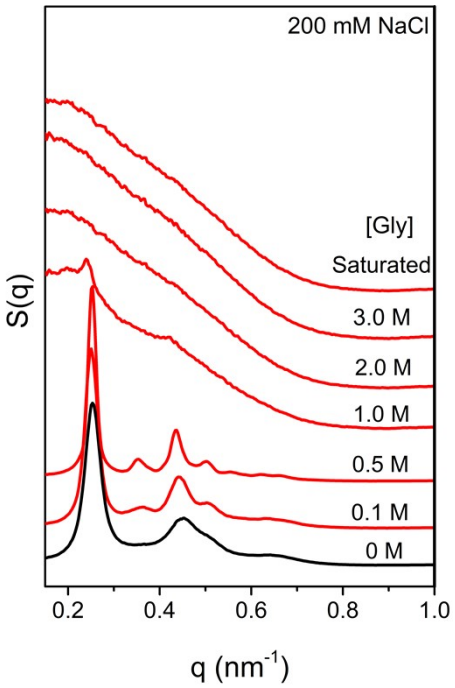

Fig. S10 SAXS data for aggregates with increasing Gly amount into 200 mM NaCl solution in the binary-component system.

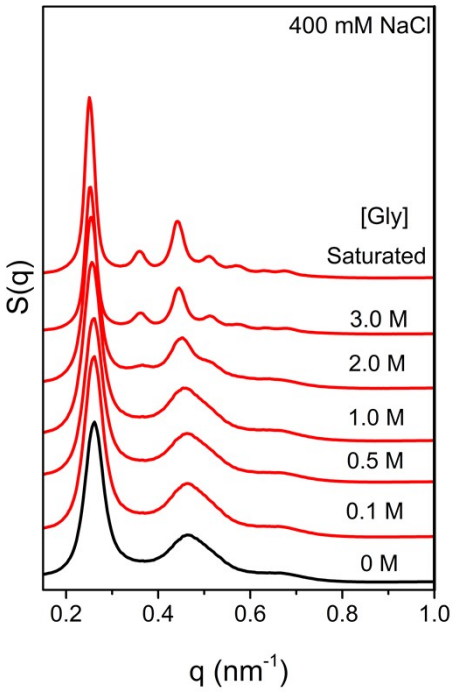

Fig. S11 SAXS data for aggregates with increasing Gly amount into 400 mM NaCl solution in the binary-component system.

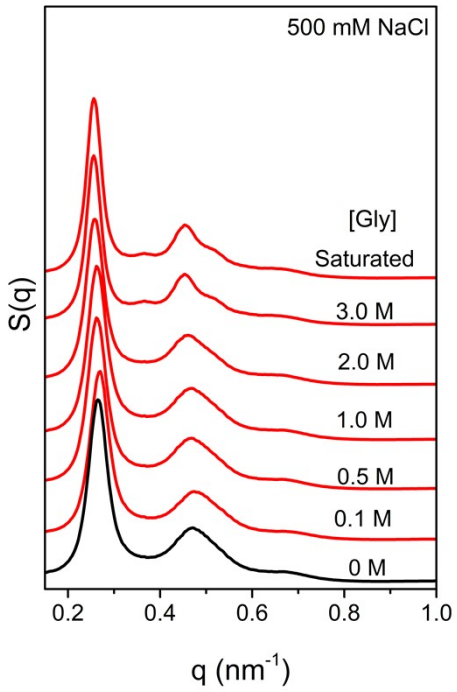

Fig. S12 SAXS data for aggregates with increasing Gly amount into 500 mM NaCl solution in the binary-component system.

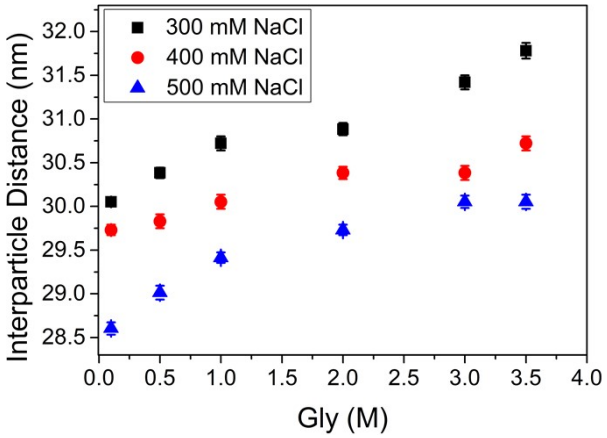

Fig. S13 The interparticle distances obtained from SAXS data in the binary-component system.

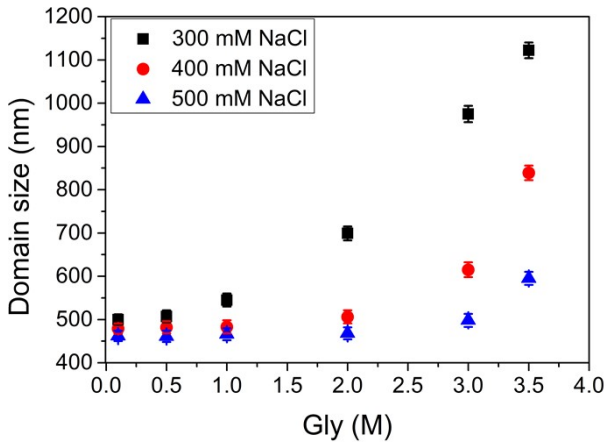

Fig. S14 The average crystalline domain sizes obtained from SAXS data in the binary-component system.

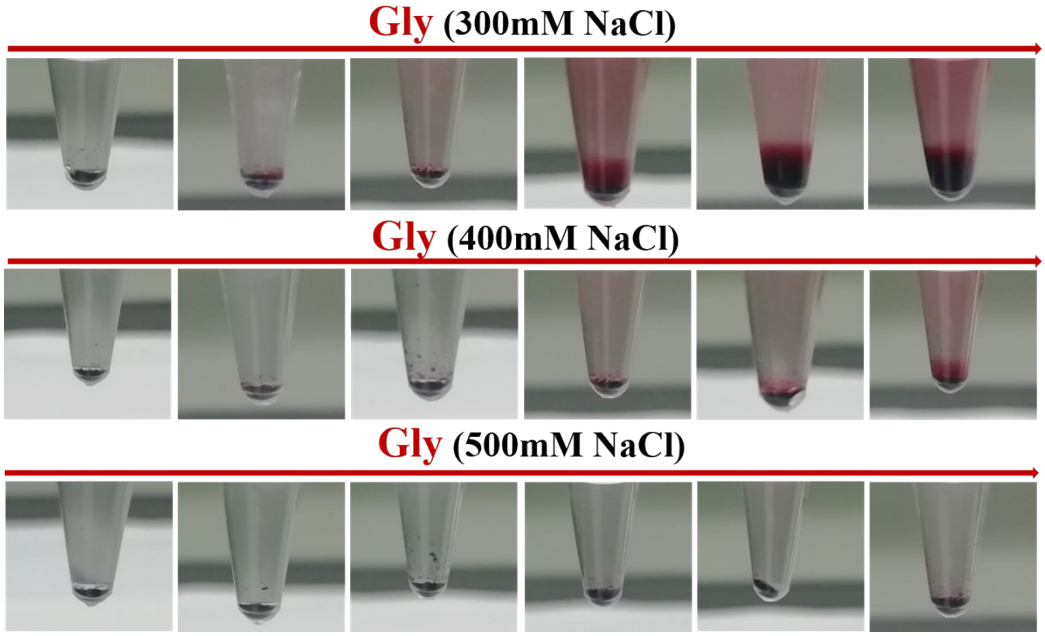

Fig. S15 The color images of aggregates in the binary-component system *via* a two-stage energy tuning strategy. From left to right, increasing Gly amount from 0.1 to 0.5 M is added into a salt solution.

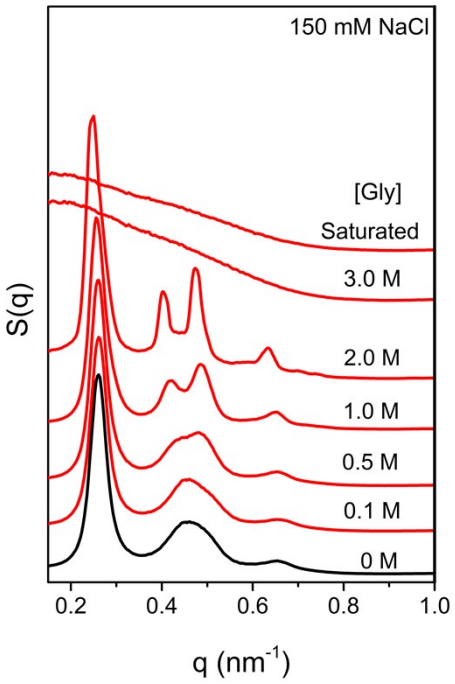

Fig. S16 SAXS data for aggregates with increasing Gly amount into 150 mM NaCl solution in the singe-component system.

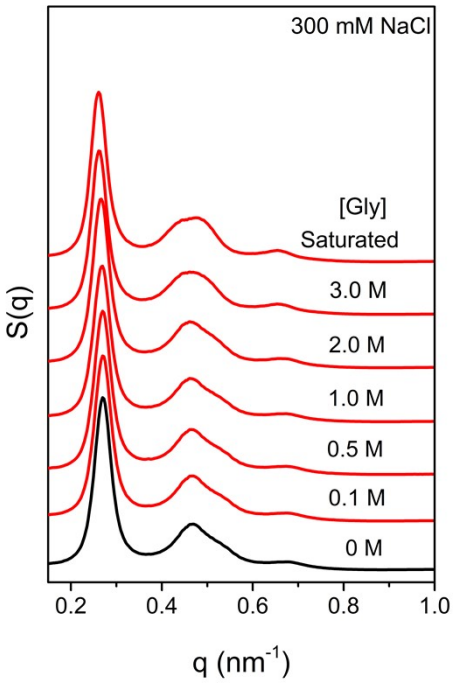

Fig. S17 SAXS data for aggregates with increasing Gly amount into 300 mM NaCl solution in the singe-component system.

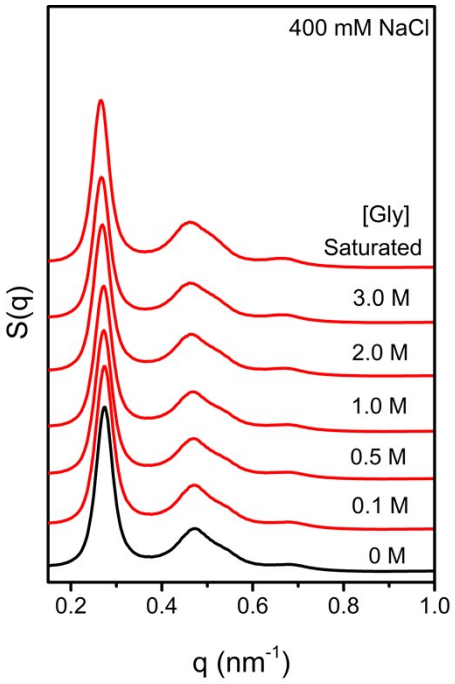

Fig. S18 SAXS data for aggregates with increasing Gly amount into 400 mM NaCl solution in the singe-component system.

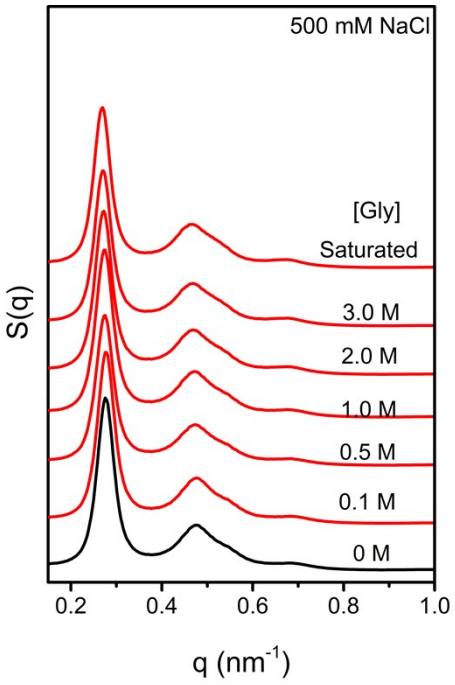

Fig. S19 SAXS data for aggregates with increasing Gly amount into 500 mM NaCl solution in the singe-component system.

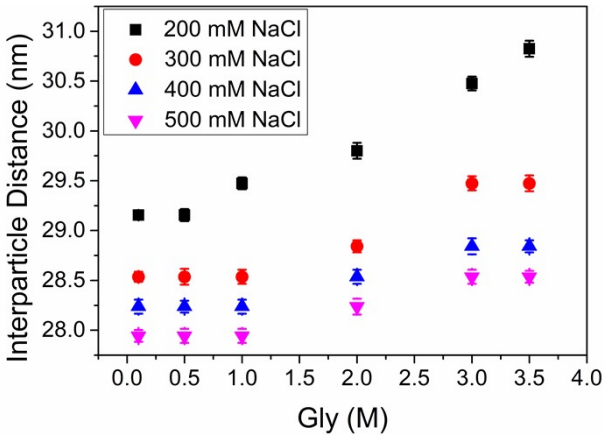

Fig. S20 The interparticle distances obtained from SAXS data in the singe-component system.

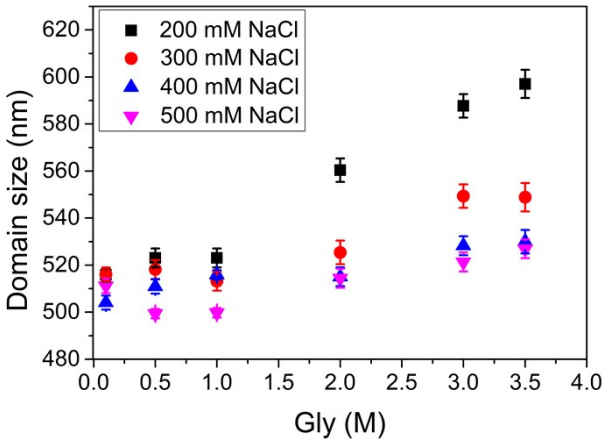

Fig. S21 The average crystalline domain sizes obtained from SAXS data in the singe-component system.

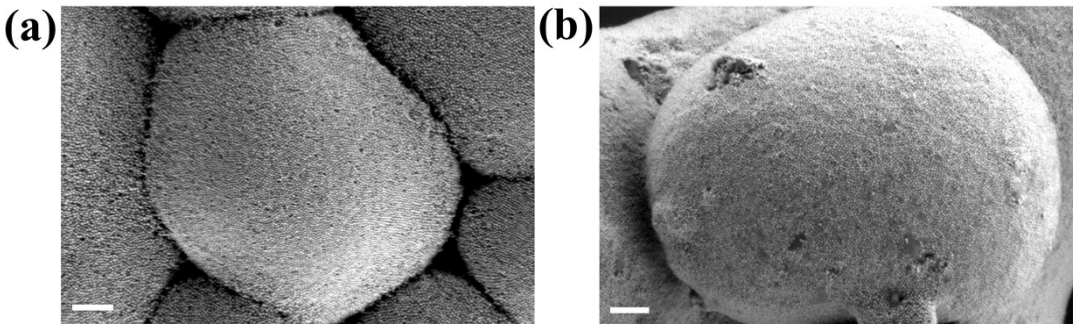

Fig. S22 SEM images of BCC crystals and FCC crystals stabilized with the DNA cross-linking reagent. Here, BCC crystals (a) and FCC crystals (b) are prepared in a saturated Gly solution (300 mM NaCl) and saturated Gly solution (200 mM NaCl), respectively. Scale bars: 200 nm.

Table S1 Element contents of DNA-functionalized gold nanoparticles obtained by EDX spectroscopy.

Element	C	N	O	P
Wt%	67.55	7.02	20.55	4.88

Table S2 DNA sequences used in this work.

DNA Type	Sequence (5' to 3')
DNA-SH	SH-AAAAAAAAAAAAGACGAATATTTAACAA
Linker -A	CGCGATTGTTAAATATTCGTCTT
Linker -X	TTCCTTATTGTTAAATATTCGTCTT
Linker -Y	AAGGAAATTGTTAAATATTCGTCTT

Table S3 Hydrodynamic diameters (d_H) of aggregates with increasing Gly amount into 300 mM NaCl solution in the binary-component system obtained from DLS.

Gly concentration	0 M	0.1 M	0.5 M	1.0 M	2.0 M	3.0 M	Saturated
d_H (nm)	344.2	449.0	454.0	767.5	1071.0	1124.5	1405.0

3. Supplementary discussion

Supplementary Note 1: According to the Manning-Oosawa condensation theory,[3] the fraction θ of DNA phosphate charges neutralized by counterions is given by:

$$\theta = 1 - \frac{1}{Z\xi} \tag{1}$$

where $\xi = l_B/b$, $l_B = q^2/4\pi\varepsilon_0\varepsilon_r kT$, b is the spacing between the phosphate charges along the chain (b=1.7Å, ξ=4.2 for native DNA in water at 20°C), l_B is the Bjerrum length, k is the Boltzmann constant, T is the absolute temperature, ε_0 is the absolute dielectric constant, ε_r is the medium dielectric constant, and Z is the counterion of valency. Therefore, the effective charge of DNA shells Q_{eff} can be derived as follows:

$$Q_{eff} = 1 - \theta = \frac{4\pi\varepsilon_0\varepsilon_r bkT}{Zq^2} \tag{2}$$

It can be concluded from this equation that Q_{eff} increases with the increase of ε_r at a constant temperature, leading to the increase of electrostatic repulsion between DNA chains and the formation of weak and reversible interactions between DNA chains, and thus providing the opportunity to adjust the assembly aggregates from disordered to highly-ordered structures.[4-7] Gly is a zwitterionic biochemical molecule, and its

addition to a solution enables an increase in the dielectric constant value of the solution.[8, 9] For instance, when 1.0 M Gly is added into a solution, the dielectric constant value can increase by 22.6.[8] In the NaCl-Gly-DNA aqueous solution, the increment of the medium dielectric constant ε_r by adding Gly will decrease the fraction of DNA phosphate charges neutralization.

Supplementary Note 2: The hydrodynamic sizes of the aggregates with increasing Gly amount into 300 mM NaCl solution are further to study by DLS measurements in the binary-component system (Fig.S8 and Table S3). Initially, the small and disordered aggregates (344.2 nm) are formed in 300 mM NaCl solution without addition of Gly. When Gly is added, their sizes gradually increase with increasing amounts of Gly in the system. At low Gly concentrations (< 3.0 M), two sizes of aggregates are observed in the system. This is probably because that a small amount of Gly induce some nanoparticles rearrange their positions to form ordered crystals, while the other nanoparticles are still locked in the initial disordered states. When Gly concentration is above 3.0 M, most nanoparticles can rearrange their positions and finally form larger crystals.

4. References

1. R. J. Macfarlane, B. Lee, H. D. Hill, A. J. Senesi, S. Seifert and C. A. Mirkin, *P. Natl. Acad. Sci. Usa.*, 2009, **106**, 10493-10498.

2. S. Lee, C. Y. Zheng, K. E. Bujold and C. A. Mirkin, *J. Am. Chem. Soc.*, 2019, **141**, 11827-11831.

3. G. S. Manning, *J. Chem. Phys.*, 1969, **51**, 924-933.

4. M. E. Leunissen, C. G. Christova, A. P. Hynninen, C. P. Royall and A. V. Blaaderen, *Nature*, 2005, **437**, 235-240.

5. O. D. Velev, *Science*, 2006, **312**, 376-377.

6. E. V. Shevchenko, D. V. Talapin, N. A. Kotov, S. O'Brien and C. B. Murray, *Nature*, 2006, **439**, 55-59.

7. D. Nykypanchuk, M. M. Maye, D. van der Lelie and O. Gang, *Nature*, 2008, **451**, 549-552.

8. S. Flock, R. Labarbe and C. Houssier, *Biophys. J.*, 1996, **70**, 1456-1465.

9. D. Baigl and K. Yoshikawa, *Biophys. J.*, 2005, **88**, 3486-3493.